J Nanostruct 16(3): 3935-3948, Summer 2026

RESEARCH PAPER

Development of a Silica- Micro/nano Biochar Hybrid System for Solid-Phase Extraction of Higenamine in Urine Samples

Fatima M. Shaker, Faiq F. Karam *, Bassam Alfarhani

Department of Chemistry, College of Science, University of AL-Qadisiyah, Iraq

ARTICLE INFO

Article History:
Received 23 March 2026
Accepted 20 June 2026
Published 01 July 2026

Keywords:
Higenamine
Human urine
Hybrid sorbent
Micro/nano Biochar
Pollution chemistry
Solid-phase extraction

ABSTRACT

The study details how to form the selective bilayer solid-phase extraction technique Higenamine concentration in human urine samples. The precipitation polymerization of methacrylic acid (MAA) and 2(dimethyl amino) ethyl methacrylate (DMAEMA) in the presence of silica ($SiO_{2)}$ particles resulted into the creation of a molecularly imprinted hybrid polymer. The most crafted substance was identified with the help of FT-IR, TGA, ^{1}H-NMR, FE-SEM, and XRD techniques to ensure the positive hybrid structure was formed and the cavities under imprint appeared inside the polymer framework. A number of experimental parameters that influenced extraction performance were optimized; these included pH of the sample, cartridge weight, percentage cartridge composing, temperature and flow rate. In ideal situations, the new technique showed a high level of linearity (R^2 = 0.9999) and low limit of detection (LOD) and limit of quantification (LOQ) indicating high sensitivity to traces of Higenamine. The imprinted polymer had a high selectivity and binding with the target compound than the non-imprinted polymer. More so; the bilayer extraction column proved to be very stable and reuseable by refining reuse a number of times without much performance being degraded. The novel procedure was effectively used to extract and determine Higenamine in human urine samples that showed good recovery and precision. In general, the presented method implies a straightforward, inexpensive yet effective method of analysis applicable both in a foresave and clinical context.

How to cite this article
Shaker F., Karam F., Alfarhani B. Development of a Silica- Micro/nano Biochar Hybrid System for Solid-Phase Extraction of Higenamine in Urine Samples. J Nanostruct, 2026; 16(3):3935-3948. DOI: 10.22052/JNS.2026.03.078

INTRODUCTION

Higenamine, chemically known as 1-[(4-hydroxyphenyl) methyl]-1,2,3,4-tetrahydroesokinin-6,7-diol, and also referred to as norcocaine, is a biologically active alkaloid that occurs naturally in many plants, such as aconite. Historically, this compound was highly valued in traditional medicine for treating systemic and non-cardiac ailments [1]. However, it has long been a significant target in forensic laboratories and other fields. Its potent role in stimulating beta-2 adrenergic receptors has led to its classification as a prohibited stimulant, warranting more attention than traditional methods [2]. The inclusion of Higenamine in matrices, its presence at low concentrations amidst a large number of major molecule metabolites, and overlapping metabolites negatively impact independent analysis [3]. and left with these limitations, the Solid-State Design (SPE) method is commonly

* *Corresponding Author Email: faiq.karam@qu.edu.iq*

used for refinement. However, this method relies on the selectivity of the adsorbent. See the published work to achieve the goal of this method: Li et al. [4] used phase methods for plant samples, although these methods often consume a large number of solvents. Members of the conference and its members [5] have diverse nano-contents, which, despite their surface area, often acquire the essential specificity of HIgenamine in complex kidneys. Furthermore, the direct photolithographic methods reviewed by Wang et al. [6] remain too expensive and complex for safe urine analysis, whereas the basic polymers used by Chen et al. [7] offer the necessary overall safety and fundamental principles. In this work, we propose a novel approach using a hybrid polymer (MIP) through precipitation. Using only the permitted materials, we aim to incorporate silica (SiO_2) into the polymer matrix during the reaction, along with a synergistic blend of MAA and DMAEMA monomers. This integration results in a robust, highly porous network where silicon dioxide (SiO_2) acts as a powerful catalyst. Simultaneously,

the deka-monomer system acts as a chemiluminescent agent, selecting Higenamine through acid-base reactions.[8] To further enhance the purification process, we employ a two-layer reactive system, utilizing an aurora lamp to boost its efficiency. Thanks to this dual system, the flooding process refreshes the eye, removing large impurities, allowing the welcoming polymer to bind effectively to the Higenamine. This integrated strategic approach to selectivity is far superior to traditional Chinese or monomeric methods.

MATERIALS AND METHODS

Higinamine hydrochloride (99.55%) was purchased from Alpha Chemical (China).KH570 (SiO_2) modified silicon dioxide nano powder (20–30 nm) was obtained from US Research Nanomaterials (USA). MAA, DMAEMA, EGDMA, and AIBN were supplied by Sigma-Aldrich (USA) for polymer synthesis, Biochar was used to prepare the two-layer solid-phase extraction.

Ciprofloxacin hydrochloride (97%) was obtained from McLean (China). All solvents, including methanol (99.9%), acetonitrile (99.9%), and glacial acetic acid, were purchased from Luba Chemie (India) and Sigma-Aldrich. All chemicals were used as is, without any processing.

Instrumentation

To verify the successful synthesis of the molecularly printed hybrid polymer, several analytical instruments were used.

Functional groups were identified using Fourier transform infrared spectroscopy (Shimadzu IR Affinity-1, Japan).

The surface morphology and distribution of silicon dioxide were characterized using field-emission scanning electron microscopy (TESCAN MIRA3, France).

For quantitative analysis of Higenamine, ultraviolet-visible spectroscopy (Shimadzu UV-1800, Japan) was used.

The structural details and other molecular interactions were confirmed using proton nuclear magnetic resonance spectroscopy (Bruker AVANCE NEO 400 MHz, Germany) with dimethyl

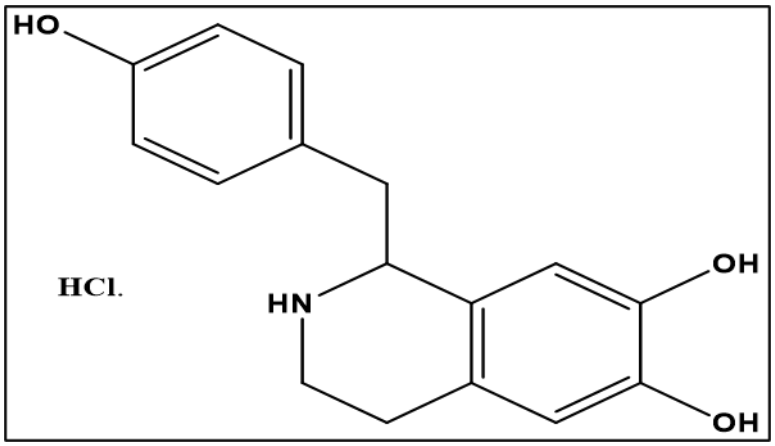

Fig. 1. Structure of Higenamine Hcl.

sulfoxide-d6 as the solvent. Additionally, the crystalline properties of the final composite were analyzed using X-ray diffraction (Shimadzu XRD-6000, Japan) with Cu-Kα alpha radiation.

Preparation and Operation of the Dual-Layer SPE Column

A 5 mL polypropylene syringe was used as the solid-phase extraction (SPE) cartridge, filled with a two-layer system (total mass: 0.50 g). The system consisted of a glass wool plug at the base, followed by a selective layer of silica-reinforced molecularly printed hybrid polymer (MIP), and a top layer of 0.20 g of pre-treated biochar. The layers were gently compacted to ensure structural stability. Prior to extraction, the column was prepared using 3 mL of high-purity methanol used for high-performance liquid chromatography (HPLC) and 3 mL of deionized water. Next, 5 mL of Higenamine was loaded by gravity. After washing, the extract was separated and quantified using UV-Vis spectroscopy at ʎ max = 285. This method followed the successful approach of the leader in reference [10].

Application to Real Human Urine Samples

processed under similar conditions to serve as a reference sample during method validation to verify the clinical feasibility of the proposed solid-phase bilayer extraction method, Higenamine levels were measured in real human urine samples. Samples were collected from a healthy

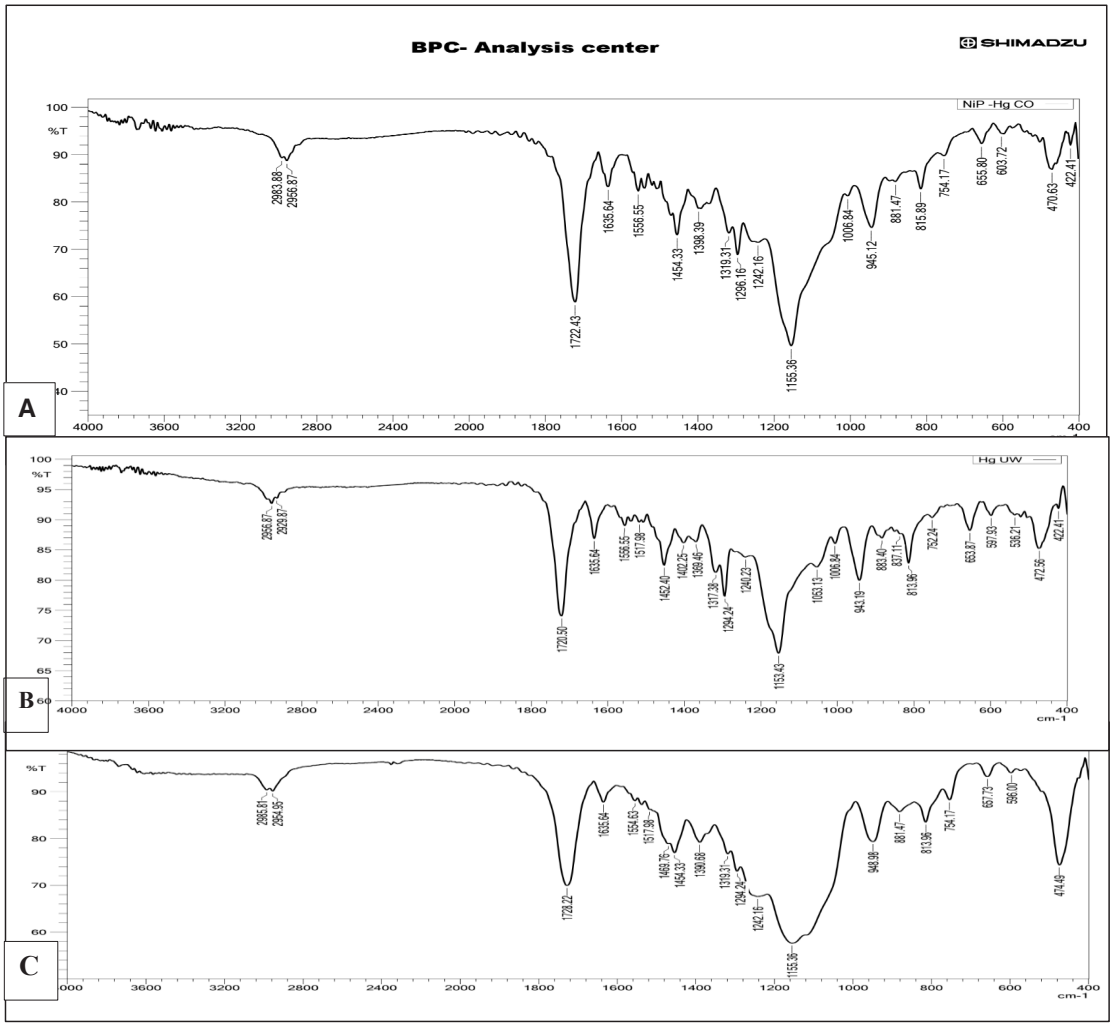

Fig. 2. Fourier transform infrared spectra of: (A) manufactured NIP, (B) Hig-loaded nanocomposite, and (C) washed MIP.

27-year-old female volunteer, in accordance with ethical guidelines and after obtaining her informed consent. To prepare the samples, protein was removed by mixing 10 mL of acetonitrile with the urine, and the sample was then centrifuged to collect the filtrate [11]. To minimize matrix effects, 7 mL of the clear filtrate was diluted with 13 mL of deionized water prior to extraction. The diluted solution was then loaded onto a bilayer column (MIP/Biochar) and analyzed using UV-Vis spectroscopy at ʎ max 285 nm. Baseline urine samples (blank samples) were processed similarly to ensure the absence of interference signals.

RESULTS AND DISCUSSION

Characterization

FTIR Spectroscopy Analysis for of the Hybrid Nanocomposites

To identify the functional groups and elucidate the chemical structure of the synthesized materials, Fourier transform infrared spectroscopy (FT-IR) was employed, and the results are shown in (Fig. 2). In the spectrum of the inorganic component (2A), the fundamental structure was confirmed by the appearance of a broad and dominant absorption band within the 1080–1100 cm^{-1} range, which is attributed to the asymmetric stretching

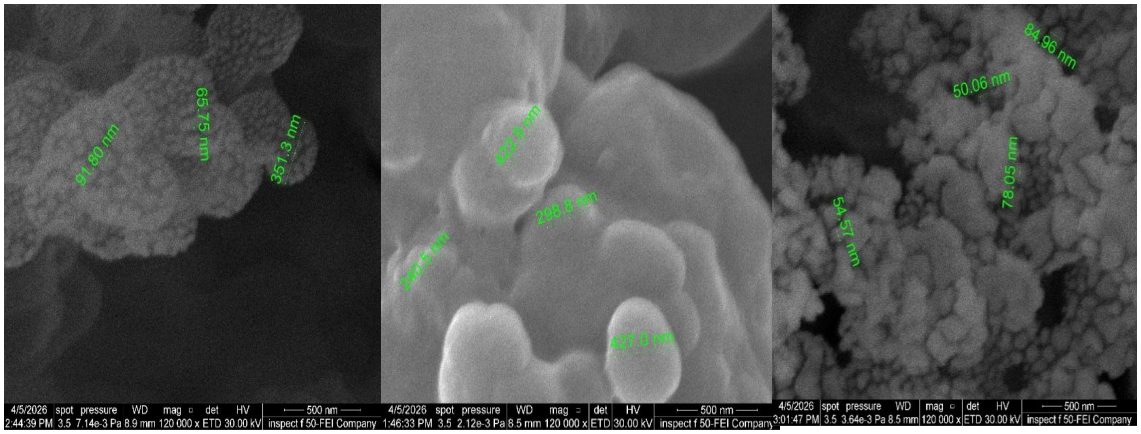

Fig. 3. Scanning electron micrographs of the hybrid polymer: (a) NIP, (b) MIP before washing, and (c) MIP after demold removal.

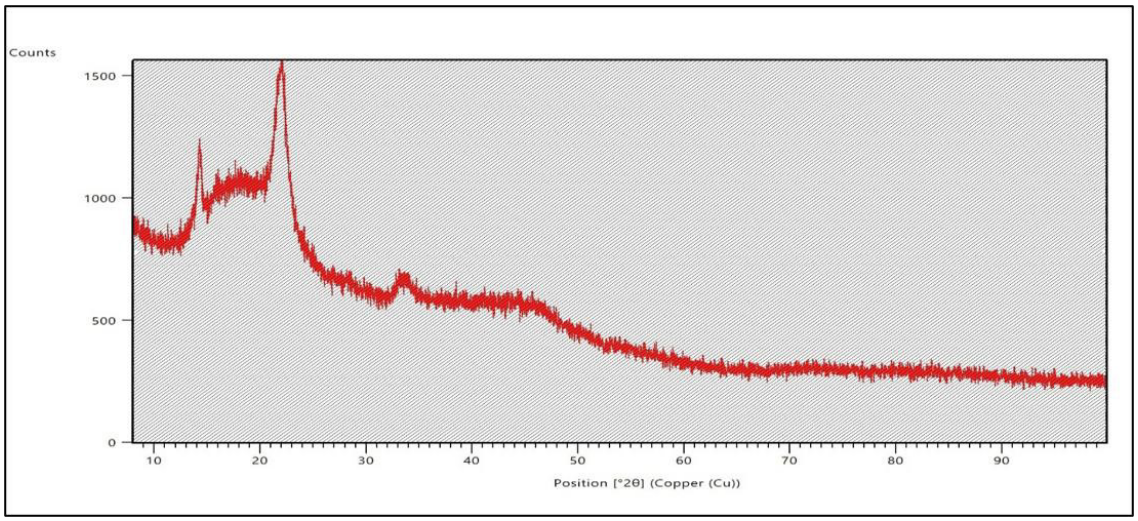

Fig. 4. Non-imprinted polymer X-ray diffraction pattern (NIP).

vibrations of the Si–O–Si bonds. Furthermore, the presence of silanol groups and structural networks was confirmed by the characteristic peaks at 950 cm^{-1} and 460 cm^{-1}, which are attributed to the Si–OH stretching and Si–O bending modes, respectively [12]. In spectrum (2B), representing the hybrid polymer prior to template removal, the successful incorporation of organic monomers is evident from the strong peak at 1730 cm^{-1} (C=O stretching in MAA and DMAEMA) and the aliphatic C–H stretching at 2950–2820 cm^{-1}. It is noteworthy that the interaction with Higenamine was confirmed by the marked broadening and peak shift in the 3400–3500 cm^{-1} range, resulting from the formation of strong hydrogen bonds and electrostatic interactions between the phenolic hydroxyl groups of the template and the carboxyl/amine groups of the functional monomers. The appearance of distinct aromatic bands in the 1500–1600 cm^{-1} range further confirms the template's encapsulation within the polymer matrix [13].

In spectrum (2C), after the leaching process, the disappearance of the template's aromatic features and the restoration of the original sharp functional group intensities indicate the complete removal of Higenamine. This demonstrates the successful formation of complementary, spatially and chemically engineered imprinted cavities. The persistence of the Si–O–Si bands in both (B) and (C) confirms the structural stability and the successful formation of a robust organic-inorganic hybrid architecture [14].

Morphological Characterization (FE-SEM Analysis)

The surface properties and morphological changes of the prepared hybrid materials were examined using Field Emission Scanning Electron Microscopy (FE-SEM), as shown in Figure 3(A–C). In (Fig. 3A), the Non-Imprinted Polymer (NIP) exhibits a course, granular morphology with high porosity. Particle sizes ranged from 65.75 nm to 91.80 nm, with some larger aggregates reaching approximately 351.3 nm. This granular nature is essential for providing a high surface area, which is a prerequisite for the efficient binding of target molecules [15]. The Higenamine-loaded, molecularly printed polymer (Fig. 3B) exhibited a denser and more compact structure compared to the un-molded polymer. Particle size increased substantially with it measuring up to 222.9 nm, 298.8 nm and 427.0 nm. The fact that this change of surface texture was accompanied by such a drastic increment in particle size is a strong indicator that the Higenamine molecules were able to fill in the imprinted cavities as well as it was able to interact with the polymer-silica matrix [16]. The surface of

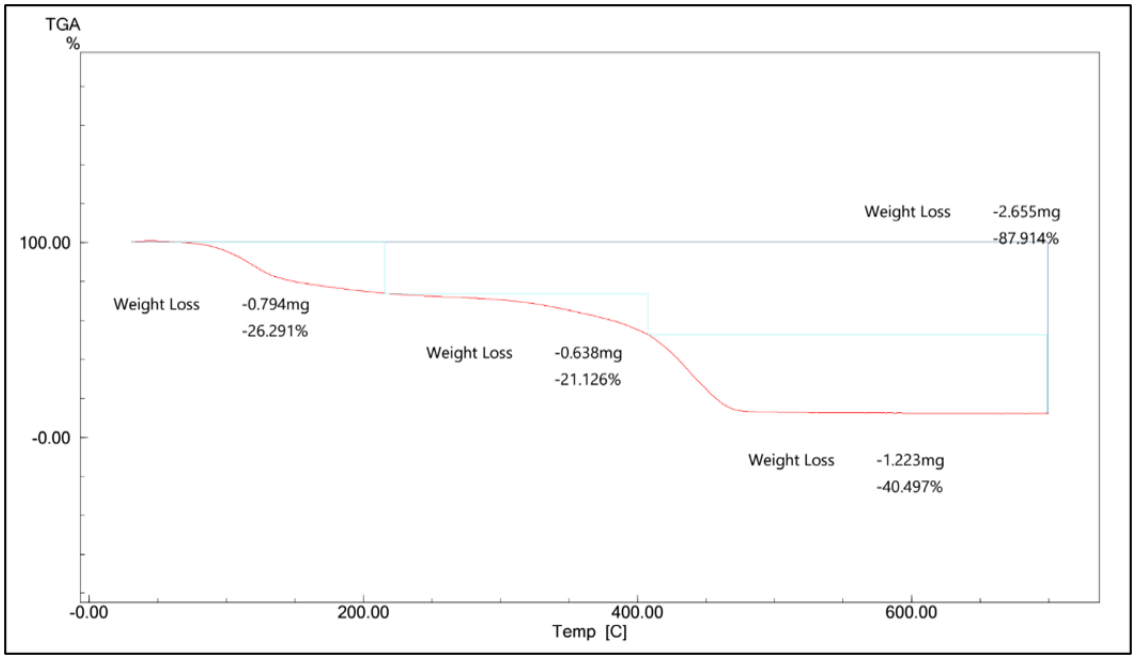

Fig. 5. Thermogravimetric analysis (TGA) curve of the synthetic non-printed nano polymer composite (NIP).

the washed and molecularly imprinted polymer (Fig. 3c) reattained its porous and irregular morphology. The particles measured were small and distinct with a diameter of 50.06 nm to 84.96 nm. The renewal of these pores and the large drop in the size of the particles over the loaded sample reports to effective template elimination leaving the easily accessible regenerated binding sites. These findings prove the structural stability of the hybrid composite and the ability to form the molecular memory on the loading and washing cycles successfully [17].

XRD Analysis

X-ray diffraction (XRD) was used to determine the crystalline structure of the hybrid material produced and determine the structural orientation (Fig. 4). The non-printed polymer (NIP) hybrid compound, in contrast to sharp Bragg reflections usually observed with crystalline monomers, is totally amorphous, as evidenced by the absence of sharp diffraction peaks. This non-crystallite

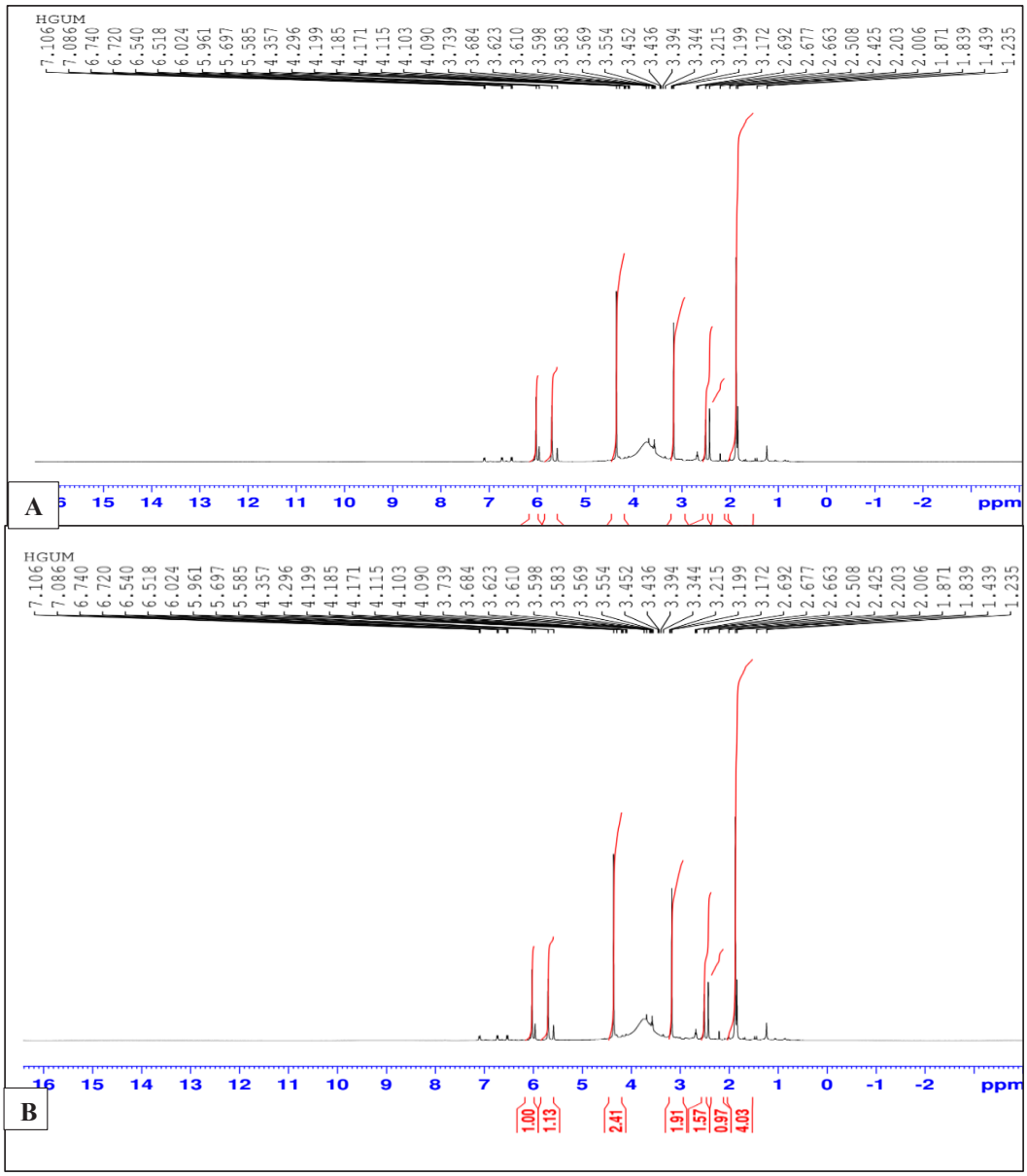

Fig. 6 Proton nuclear magnetic resonance (^{1}H NMR) spectra of (a) non-printed polymer (NIP) and (b) Higenamine template.

form is very favorable to the columns of extraction constructed, it giving a greater porosity and accessibility to the internal structure. This enables the free diffusion of the Higenamine molecules and gives them the ability to interact effectively with the binding sites to be loaded and extracted. In addition, the large width of the diffraction lines proves the successful crosslinking of both the MAA and DMAEMA strands with the silica network to produce a stable and uniform hybrid structure devoid of crystalline contaminants [18].

Thermogravimetric Analysis (TGA)

The last decomposition process is done at higher temperatures than 450 ˚C and the final weight loss is 40.49% This step is associated with the total breakdown of the polymer network cross links. The mass left unaffected is stable to a temperature of

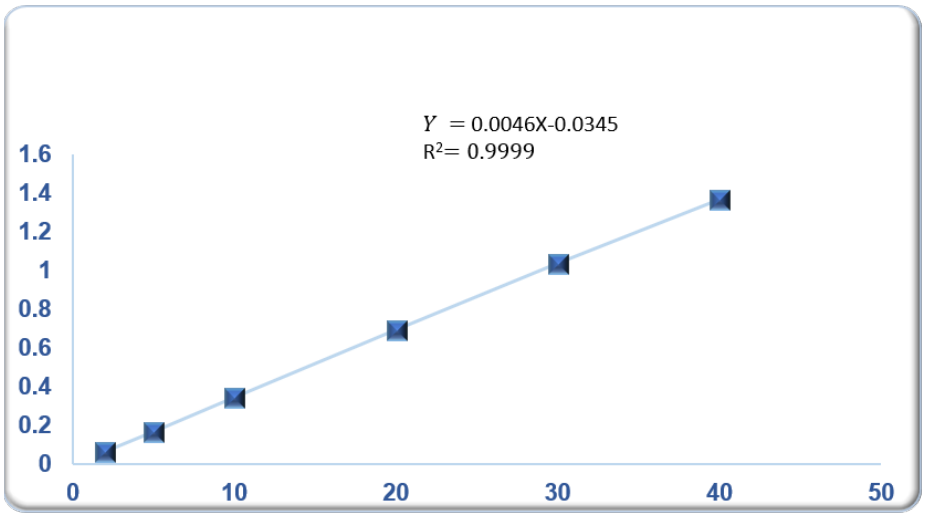

Fig. 7: Calibration chart for determining the amount of Higenamine.

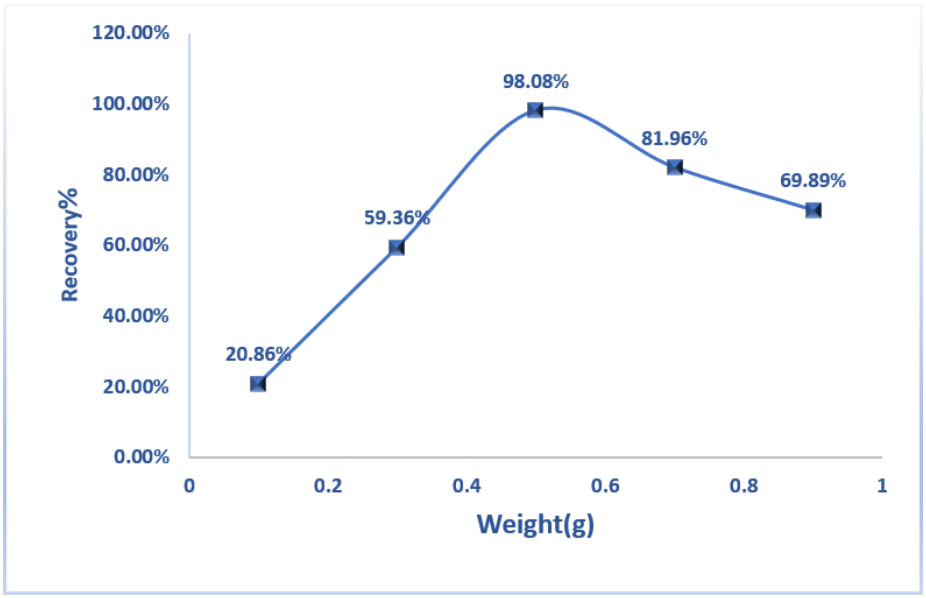

Fig. 8. Improving cartridge mass for Higenamine extraction.

700 ˚C and this is a testament to the fact that there is an inorganic silica (Sio $_2$) structure. Adding silica to the composite increases the thermal stability of the material since it creates a thermal shield that supports the structural integrity of the material at high temperatures. These findings suggest that the hybrid material is highly thermally stable and can be employed in analytic applications without decreasing in thermal stability [19].

^{1}H NMR Analysis

To confirm the chemical composition and the success of the molecular imprinting process, proton nuclear magnetic resonance (^{1}H NMR) spectra were recorded for both the imprinted polymer (NIP) and the Higenamine template, as shown in Figures 6(A) and 6(B). The spectrum of the unprinted polymer (NIP) (Fig. 6A) shows characteristic aliphatic signals between 0.87 and 1.87 ppm, which represent the main-chain protons of the polymer (methyl and methylene groups). Furthermore, the observed peaks around 3.04 – 4.35 ppm are attributed to the functionalized monomer units, confirming the successful copolymerization of the organic matrix.

In comparison, the spectrum of the Higenamine-loaded imprinted polymer (Fig. 6B) shows characteristic aromatic protons in the low chemical shift region, specifically between 6.51 and 7.10 ppm, a feature characteristic of the aromatic rings in the Higenamine molecule. We also observed the characteristic signals of the drug's tetra hydro iso quinoline ring at 2.66 – 3.68 ppm.

Comparison of the two spectra confirms the presence of the major functional groups of both the polymer matrix and the drug in the final composite. The slight shifts in proton positions when comparing the pure drug to the integrated system indicate successful molecular interactions) hydrogen bonding and electrostatic forces) between the Higenamine and the host cavities

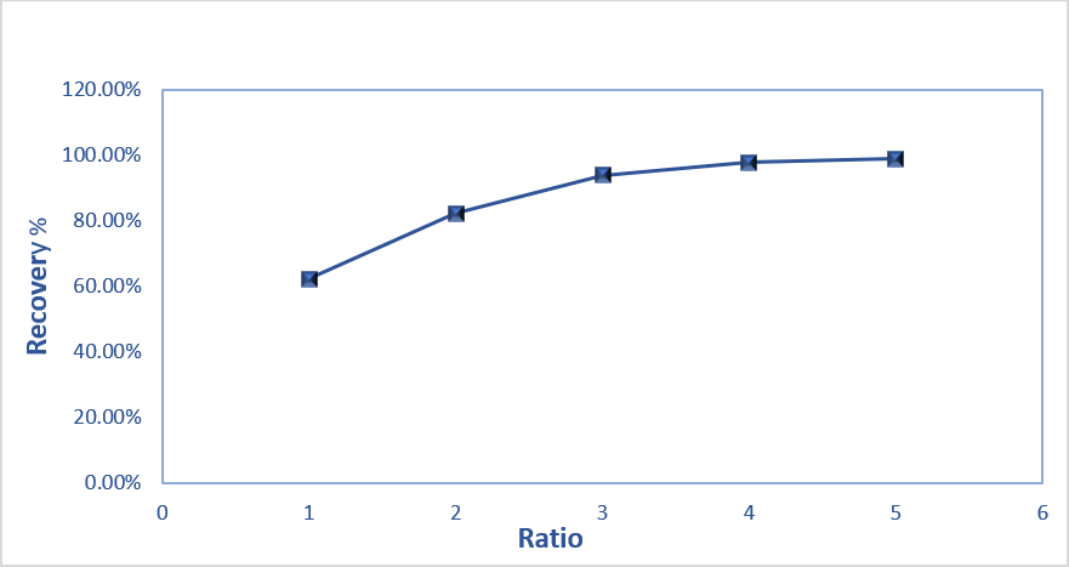

Fig. 9. Effect of MIP/Biochar composition on Higenamine extraction.

Table1 Components percentage of cartridge.

Sample Number	Mix (MIP) (g)	Biochar (g)	Total Mass (g)	Absorbance	Recovery (%)
1	0.25	0.25	0.5	0.8462	62.29%
2	0.225	0.275	0.5	0.9631	75.40%
3	0.29	0.21	0.5	1.1025	88.15%
4	0.275	0.225	0.5	1.2401	97.67%
5	0.3	0.2	0.5	1.321	98.84%

Nuclear magnetic resonance (NMR) data, together with previously obtained Fourier transform infrared (FT-IR) results, provide strong evidence for the successful formation of the molecularly imprinted structure [20].

Calibration Curve and Validation of the Method

In order to determine the linearity of the analytical procedure, a calibration was plotted out as seen in (Fig. 7) that shows the relationship between absorbance and the various Higenamine concentrations. Excellent linearity was achieved within a concentration range of 2–40 µg.mL^{-1}. The regression equation resulted as: y = 0.0046x -0.0345, the y being the absorbance and the x the Higenamine concentration. The high R is attributed to the fact that the correlation coefficient (R^2 = 0.9999) value is extremely high which clearly shows the high degree of reliability and sensitivity of the method in the accurate determination of

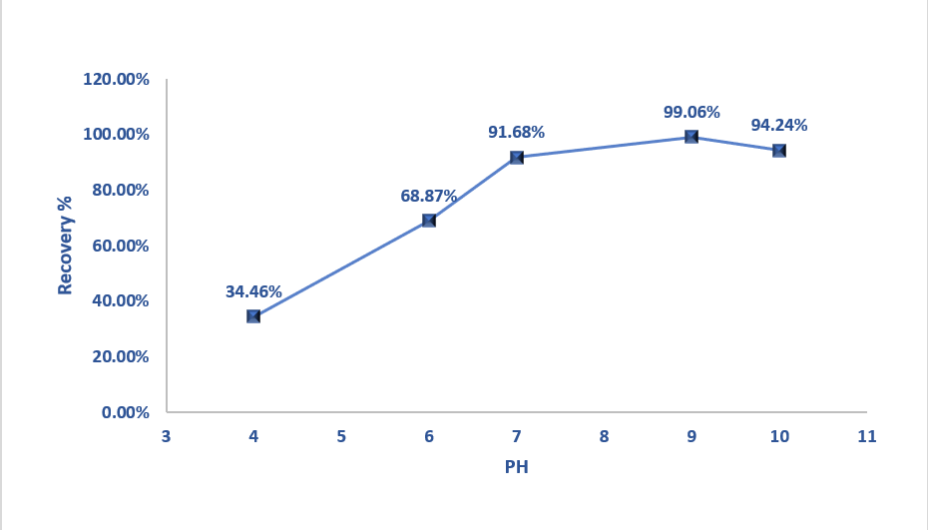

Fig. 10. Effect of solution pH on Higenamine extraction.

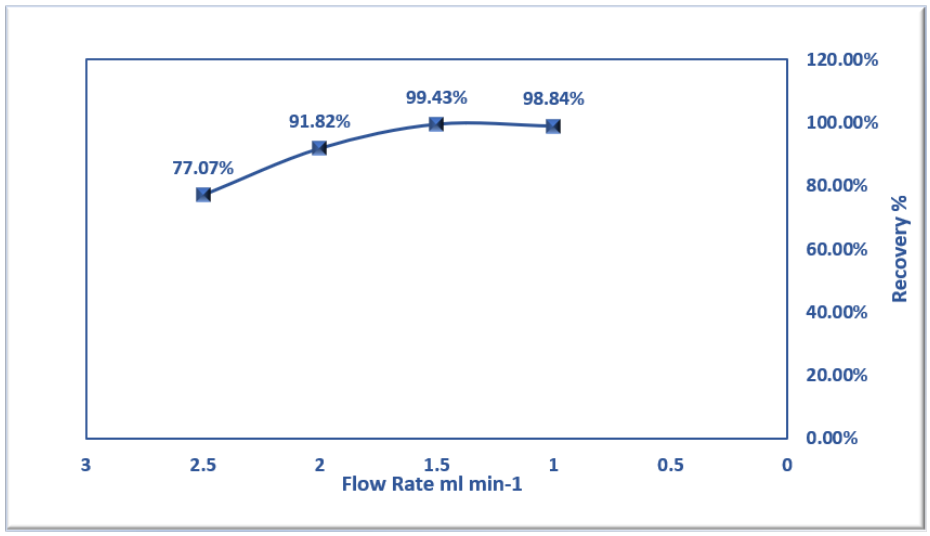

Fig. 11. Impact of sample flow rate on the Recovery %.

the analyte. Moreover, sensitivity was ascertained by the determination of the limit of detection and the limit of quantification, which were 0.358 $\mu g.mL^{-1}$ and 1.086 $\mu g.mL^{-1}$, respectively. These statistical values prove that the created method has a high level of analytical functions and can be used to determine the level of Higenamine in different samples quantitatively.

Optimization of Extraction Conditions

Optimization of Cartridge Weight

The quantity of sorbent in the cartridge directly influences the total extraction capacity and available surface area, and is therefore an important factor that must be optimized. In the experiment, the impact of the mass of the sorbent was analyzed with dissimilar weights (0.1, 0.3, 0.5, 0.7 and 0.9 g) to decide on the best conformity of the DMAEMA/silica/MAA compound hybrid layer. Fig. 8 shows that the Higenamine extraction efficiency rose with the mass of the sorbent peaking at 98.08% at 0.5 g. This can be explained by the number of active sites and cavities that have been imprinted to interact with the analyte. Nevertheless, even at a sorbent mass of more than 0.5 g (0.7 and 0.9 g) the extraction efficiency was gradually decreasing. This is typical with solid-phase extraction systems and is mostly attributed to the fact that the process can have a higher mass transfer resistance because the layer of sorbent becomes thicker [21]. In this case, the penetration of the solvents will be inefficient and may result in the inability to reach the active sites as well as causing uneven distribution of the flows within the cartridge. According to these results, 0.5 g was chosen as the best mass of sorbent to use in further experiments in order to provide a good mass transfer and a constant extraction work [22].

Effect of Cartridge Component Ratio

To improve extraction efficiency, different mass ratios of the hybrid matrix components (MAA/DMAEMA/Sio_2) and biochar were investigated, as summarized in (Table 1). The integration of the biochar layer with the molecularly imprinted polymer (MIP) within the cartridge plays a crucial role in increasing the surface area and providing additional active sites for Higenamine adsorption. As shown in Fig. 9, the extraction efficiency gradually increased from 62.29% to a maximum of 98.84% at ratio 5 (0.3 g of MIP and 0.2 g of biochar). This behavior is attributed to the synergistic effect between the MIP layer and the biochar material. The MIP provides selective discrimination through the printed cavities, while the biochar contributes a porous structure that facilitates the diffusion of Higenamine molecules. The slight difference in extraction efficiency between ratio 4 (97.67%) and ratio 5 (98.84%) indicates that the system approached optimal performance. In addition, the balanced structure helped avoid excessive crosslinking density that could limit the diffusion

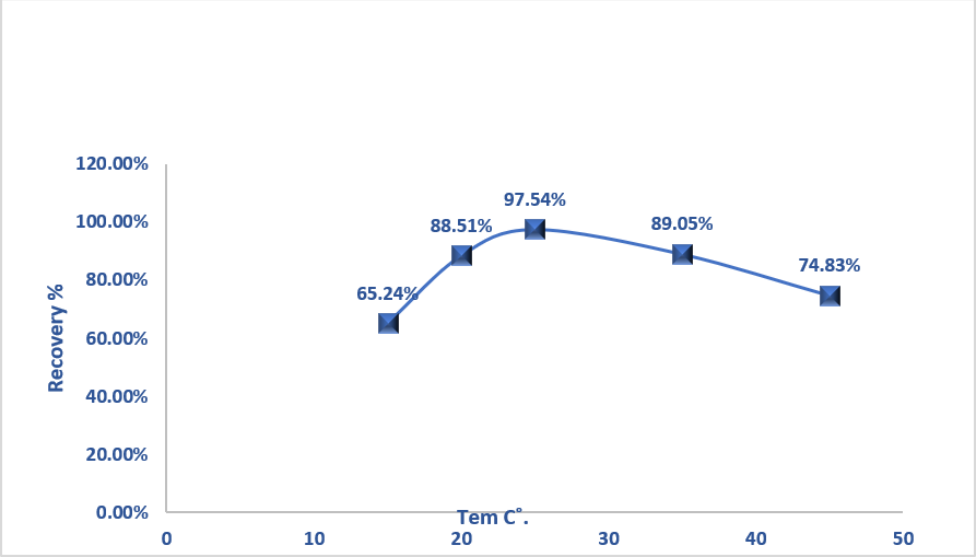

Fig. 12. Influence of temperature on Recovery % of Higenamine.

of molecules, while maintaining sufficient carboxyl and amine functional groups for hydrogen bonding and electrostatic interactions. To Accordingly, ratio 5 was determined to be the optimal configuration for all subsequent analytical tests [23,24].

Effect of pH on Sample Solutions

The pH of the aqueous medium is a crucial factor in solid-phase extraction (SPE), as it determines the degree of ionization of Higenamine molecules and their interaction with the surface of the adsorbent. The pH of the samples was adjusted between 4.0 and 10.0 to achieve optimal conditions, as shown in (Fig. 10) and Fig. 10. A pH of 9.0 was found to achieve the highest extraction efficiency of 99.06%. At this alkaline pH, strong electrostatic interactions occur between the Higenamine molecules and the functional groups of the hybrid matrix. This results in a strong electrostatic attraction that facilitates the entry of the drug molecules into the formed cavities [25], where they are further stabilized by hydrogen bonds. However, raising the pH to 10.0 resulted in a decrease in the extraction efficiency to 78.84%. This decrease is most likely due to the loss of protons from the active sites on the adsorbent, resulting in electrostatic repulsion between the surface and the drug molecules. Consequently, pH 9.0 was chosen as the optimal value for maximum extraction capacity.

Effect of Sample Flow Rate on Higenamine Extraction

Sample flow rate is another important factor in the extraction process, as it determines the contact time between the Higenamine molecules and the absorbent layer. Flow rates ranging from 0.5 to 2.5 mL.min^{-1} were evaluated. As shown in (Fig. 11), the highest extraction efficiency was achieved at a flow rate of 1.5 mL.min^{-1}, reaching 99.43%. At lower flow rates (0.5 and 1.mL.min^{-1}), the extraction efficiency decreased slightly, while a significant decrease was observed at higher flow rates, reaching 73.10% at 2.5 mL.min^{-1}. This behavior is attributed to the sample's residence time within the cartridge. At a flow rate of 1.5 mL.min^{-1}, sufficient reaction time is available for the Higenamine molecules to effectively interact with the printed cavities and functional groups. At higher flow rates, the molecules pass rapidly through the column, resulting in insufficient contact time for effective binding to the active sites. To balance a high extraction rate with rapid analytical performance, 1.5 mL.min^{-1} was determined as the optimal flow rate for all subsequent experiments, ensuring maximum efficiency without unnecessary time loss [26].

Effect of temperature on Higenamine extraction

We observed high extraction efficiency within a temperature range of 15–45 °C, as shown in (Fig.

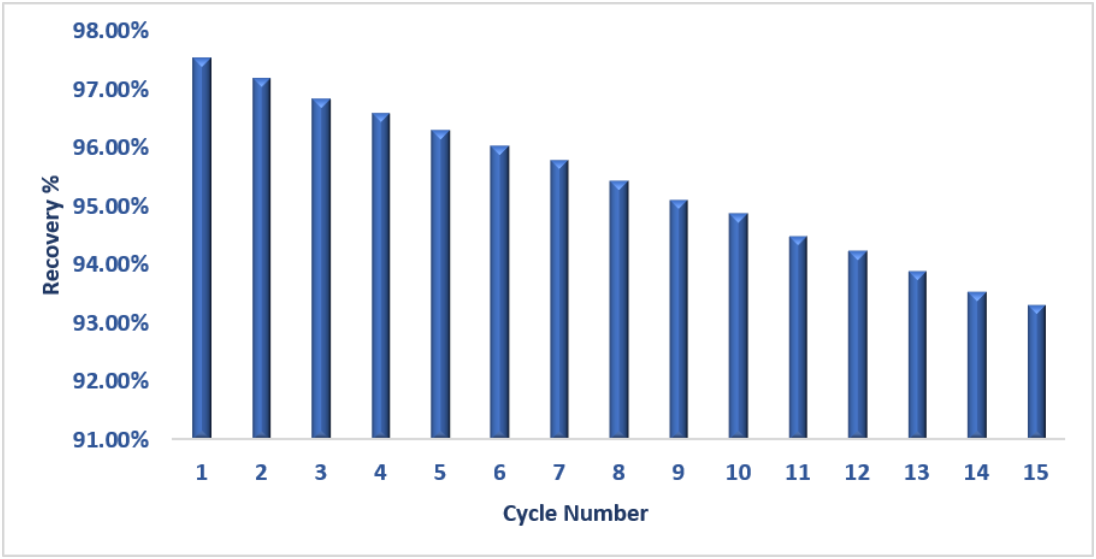

Fig. 13. Stable performance of the MIP column during repeated use.

12). Optimal performance was observed at 25 °C (room temperature), where the highest extraction rate reached 97.54%. However, the extraction rate gradually decreased with increasing temperature, reaching its lowest levels at 35 and 45 °C. This indicates that the adsorption of Higenamine onto the hybrid compound is an exothermic reaction [27]. This decrease in efficiency is likely due to two main factors: first, the adsorbed molecules gain sufficient thermal energy to release and return to the liquid state; and second, the electrostatic forces and hydrogen bonds between the analyte and the adsorbent surface may weaken at higher temperature .The significance of these results lies in the fact that the developed method exhibits high efficiency at room temperature, eliminating the need for additional heating or cooling, thus making it more cost-effective and suitable for routine analytical procedures.

Analytical Performance: Imprinting Factor, Detection Limit, and Quantity Limit

To evaluate the efficiency and sensitivity of the MIP-SPE method developed for Higenamine analysis, the imprinting factor (IF), detection limit (LOD), and quantity limit (LOQ) were defined and calculated theoretically.

The imprinting factor (IF) represents the relative affinity of the molecularly imprinted polymer (MIP) towards the template molecule compared to the non-imprinted polymer (NIP), and is and was found to be 6.18, as determined by Eq. 1:

$$\mathrm{IF} = \frac{\mathrm{RMIP}}{\mathrm{RNIP}} \quad (1)$$

Where R_{MIP} and R_{NIP} represent the recovery ratios of printed and unprinted polymers, respectively. Under the optimal conditions, the extraction recovery of the Nip was found to be 16.09%With MIP recovery of 99.43%, the calculated IF value was 6.18, indicating that MIP possesses important molecular recognition sites and a much higher affinity for Higenamine compared to the unprinted polymer. sensitivity of the analytical procedure was evaluated using the limit of detection (LOD) and the limit of quantity (LOQ). In accordance with the recommendations of the International Union of Pure and Applied Chemistry (IUPAC), these limits are based on the standard deviation of the blank sample (δ) and the slope of the calibration curve (S), as shown in the following two mathematical Eqs. 2 and 3.

$$\mathrm{LOD} = \frac{3.3.\delta}{\mathrm{S}} \quad (2)$$

$$\mathrm{LOQ} = \frac{10.\delta}{\mathrm{S}} \quad (3)$$

The calibration curve Higenamine showed excellent linearity within a concentration range of 2.0 to 40.0 $\mu g.mL^{-1}$, with an excellent correlation coefficient R^2 of 0.9999 and a regression equation y = 0.0046x - 0.0345. Based on these calculations, the limit of detection (LOD) and limit of quantity (LOQ) were found to be 0.358 $\mu g.mL^{-1}$ and 1.086 $\mu g.mL^{-1}$, respectively Finally, the accuracy of the developed procedure was verified by determining the relative standard deviation (RSD) across five consecutive measurements (n = 5). The results obtained confirmed the robustness and reliability of the proposed method for analyzing of Higenamine in complex matrices.

Reusability and Stability of the MIP Column

Practically and financially, efficiency of MIP-SPE column being reusable is another vital aspect of determining performance of the method. The stability of the formed hybrid composite was tested during 15 successive loading and washing steps with the help of a proper regenerating solvent that eliminates the amounts of left template particles. According to (Fig. 13), the synthesized MIP proved to be highly stable with the initial recovery value being 97.54% under the optimum conditions. Repeated cycles led to a slight fall in extraction efficiency, possibly because of the slow saturation of active binding sites or a slight change in polymer matrix structure. But the recovery rate was 93.10% through fifteenth cycle signifying acceptable stability on repeated usage. The recovery loss was lower than 5 percent, which proved the stability of the printed cavities both mechanically and chemically. These findings indicate that the completed MIP-SPE column can be re-used severally without serious deterioration in the analytical ability and hence it can be ranged to perform regular Higenamine analysis [28].

Analysis of Real Samples and Evaluation of Matrix Effects

The MIP-SPE technique was tested clinically through evaluating Higenamine extraction using

two media Pure methanol and a normal human urine sample. The findings indicated that the extraction rate in pure methanol was at 99.43 that was in line with optimized experimental conditions. Conversely, the extraction efficiency in the biological medium was slightly reduced with a recovery rate of 95.60% in normal human urine samples. This reduction has been suggested to be due to the effect of the matrices because compounds like urea, salts, and proteins, can be competing against Higenamine as regards the imprinted recognition sites. However, the method-maintained recovery rates exceeding 95% with small relative standard deviations (n=5), attest to its high level of strength and effectiveness in thick bioanalytical usage. These findings reveal the usefulness of the produced MIP/biochar composite in the selective extraction of Higenamine on actual, patient samples.

Validity Methods: Accuracy, Precision and Robustness

The efficiency of the developed MIP-SPE technique was approved by the internal and external accuracy tests on a concentration of 20 $\mu g.mL^{-1}$ (n=5). The findings were very accurate with an intraday relative deviation of 1.24% and inter-day relative deviation (calculated by three successive days) of below 1.92%. Besides the high recovery values of the method of more than 97, the strength of the method was also tested on the introduction of small, but deliberate change in operating conditions, including flow rate (+ =0.1 $mL.min^{-1}$) and the quantity of the solvent adding (+ =0.2 ml). The recovery of Higenamine was also found to be very stable with a percentage deviation of less than 1.5 suggesting that the technique is not sensitive to in vitro variations. Moreover; stability measurements showed that the analyte could be kept in the matrix at room temperature of 40C and at not more than 7 days without any apparent degradation with a degradation rate of below 1.6. In this way, the validity, efficiency and applicability of the proposed method in time-routinely analyzing Higenamine in pharmaceutical and clinical use is confirmed, even under the circumstances where a sample cannot be processed in real time.

CONCLUSION

This study aimed to prepare a biochar-bound molecularly imprinted composite (MIP) with selective properties for use with Higenamine, using solid-phase extraction (SPE). Typical optimum conditions included 0.5 g of the material, pH 9.0, temperature 25 °C, and a flow rate of 1.5 mL min^{-1}. $\mu g\ mL^{-1}$ Under these conditions, the maximum extraction rate reached approximately 99·43% in the artificial medium· The MIP/biochar system outperforms previous methods due to its wide linearity range (2·0–40·0 $\mu g\ mL^{-1}$), high fingerprint index (IF =), and high sensitivity· Both the total limit of detection (LOD) of 0·358 $\mu g\ mL^{-1}$ and the limit of quantity (LOQ) of 1·086 $\mu g\ mL^{-1}$ are lower than many conventional solid-phase extraction methods, indicating that the addition of biochar significantly improves the system›s efficiency and surface area· Among the methods studied, a sustainable and effective approach to minimizing matrix effects in complex biological samples was employed. This method demonstrated good performance in real human urine samples, indicating its suitability for application in routine clinical and forensic analyses.

CONFLICT OF INTEREST

The authors declare that there is no conflict of interests regarding the publication of this manuscript.

REFERENCES

1. Jing Z, Qiang W, Chen-Ming F, Xiaofan Y, PengYi T, Bing L. Author response for "$ZnIn_2S_4$-based heterostructure photocatalysts for solar energy conversion: A comprehensive review". Royal Society of Chemistry (RSC); 2025.
2. Read D, Skinner J, Lock D, Smith ACT. The creation of the World Anti-Doping Agency. WADA, the World Anti-Doping Agency: Routledge; 2021. p. 39-62.
3. Phung K. LC-MS techniques for analytical testing of recombinant human erythropoietin and darbepoetin alfa in equine plasma samples for anti-doping control: Iowa State University.
4. Xiao-wei H, Zhi-hua L, Xiao-bo Z, Ji-yong S, Han-ping M, Jie-wen Z, et al. Detection of meat-borne trimethylamine based on nanoporous colorimetric sensor arrays. Food Chem. 2016;197:930-936.
5. Zhao Y, Yavari K, Liu J. Critical evaluation of aptamer binding for biosensor designs. TrAC, Trends Anal Chem. 2022;146:116480.
6. Thomas A, Geyer H, Guddat S, Schänzer W, Thevis M. Dried blood spots (DBS) for doping control analysis. Drug Testing and Analysis. 2011;3(11-12):806-813.
7. Li G, Row KH. Recent Applications of Molecularly Imprinted Polymers (MIPs) on Micro-extraction Techniques. Separation and Purification Reviews. 2017;47(1):1-18.
8. Martín-Esteban A. Molecularly Imprinted Polymers: Providing Selectivity to Sample Preparation. Molecularly Imprinted Polymers for Analytical Chemistry Applications: The Royal Society of Chemistry; 2018. p. 379-411.

9. Arabi M, Ostovan A, Ghaedi M, Purkait MK. Novel strategy for synthesis of magnetic dummy molecularly imprinted nanoparticles based on functionalized silica as an efficient sorbent for the determination of acrylamide in potato chips: Optimization by experimental design methodology. Talanta. 2016;154:526-532.
10. Hu T, Chen R, Wang Q, He C, Liu S. Recent advances and applications of molecularly imprinted polymers in solid-phase extraction for real sample analysis. J Sep Sci. 2021;44(1):274-309.
11. Javanbakht M, Shaabani N, Abdouss M, Ganjali M, Mohammadi A, Norouzi P. Molecularly Imprinted Polymers for Selective Solid-Phase Extraction of Verapamil from Biological Fluids and Human Urine. Current Pharmaceutical Analysis. 2009;5(3):269-276.
12. Bagheri AR, Arabi M, Ghaedi M, Ostovan A, Wang X, Li J, et al. Dummy molecularly imprinted polymers based on a green synthesis strategy for magnetic solid-phase extraction of acrylamide in food samples. Talanta. 2019;195:390-400.
13. Ya-Li H, Wei-Ming C, Xiao-Zhang F. The alkaloids of Melodinus morsei. Phytochemistry. 1994;37(4):1055-1057.
14. Soon-gil K, In-jae L, Sang-gon K, Jun-phill E, Jin-gyeong P, Sun-mi L, et al. Enhancing the solar cell efficiency with optimized metal paste. 10th IEEE International Conference on Nanotechnology; 2010/08: IEEE; 2010. p. 1151-1155.
15. Saleh TA. Surface and morphological characterization of hybrid materials. Polymer Hybrid Materials and Nanocomposites: Elsevier; 2021. p. 241-283.
16. Zhou J, Wang Y, Ma Y, Zhang B, Zhang Q. Surface molecularly imprinted thermo-sensitive polymers based on light-weight hollow magnetic microspheres for specific recognition of BSA. Appl Surf Sci. 2019;486:265-273.
17. Kumar Shee N, Kim H-J. Complementary metalloporphyrin-based nanostructure decorated with silver nanoparticles for photocatalytic degradation of organic dyes. Inorg Chem Commun. 2024;163:112252.
18. Costa ROR, Lameiras FS, Vasconcelos WL. Structural Control in Poly(butyl acrylate)-Silica Hybrids by Modifying Polymer-Silica Interactions. J Sol-Gel Sci Technol. 2003;27(3):343-354.
19. Chylińska M, Kaczmarek H. Thermal degradation of biocidal organic N-halamines and N-halamine polymers. Thermochim Acta. 2014;583:32-42.
20. Maheshwari S, Kaur K, Kaur S, Malik AK. Advancements in Molecularly Imprinted Polymer-Based Electrochemical Sensors: Fabrication, Functionalization, Applications, and Future Perspectives. Molecularly Imprinted Polymers: Path to Artificial Antibodies: Springer Nature Singapore; 2024. p. 245-272.
21. Zhao X, Zhang R, Li Q, Liu Y, Zhang Z, Zeng Y, et al. $Ti_3C_2T_x$-bonded aminopropyl-modified spherical silica: A novel dispersive solid-phase extraction sorbent for determination of 9 fluoroquinolones. Microchem J. 2025;219:116060.
22. Yılmaz H, Basan H. Development of a molecularly imprinted solid-phase extraction sorbent for the selective extraction of telmisartan from human urine. J Sep Sci. 2015;38(8):1433-1439.
23. Han X, Han X, Bo S, He Y-C, Yang S. Biochar-Based Surface Molecularly Imprinted Polymers for Selective Separation of Camptothecin. Elsevier BV; 2025.
24. Wu G, Wang Z, Wang J, He C. Hierarchically imprinted organic–inorganic hybrid sorbent for selective separation of mercury ion from aqueous solution. Anal Chim Acta. 2007;582(2):304-310.
25. Zhao X, Guo Z, Yang H. Molecularly imprinted polymer composites in food analysis. Molecularly Imprinted Polymer Composites: Elsevier; 2021. p. 345-380.
26. Yang R, Liu Y, Yan X, Liu S. Simultaneous extraction and determination of phthalate esters in aqueous solution by yolk-shell magnetic mesoporous carbon-molecularly imprinted composites based on solid-phase extraction coupled with gas chromatography–mass spectrometry. Talanta. 2016;161:114-121.
27. Shi L, Qiu J, Wang W, Ding Z, Zhang W, Liang J, et al. Influence of cations and low molecular weight organic acids on Cs(I) adsorption on montmorillonite and vermiculite. J Mol Liq. 2024;402:124778.
28. Collinson MM. Imprinted Functionalized Silica. The Supramolecular Chemistry of Organic-Inorganic Hybrid Materials: Wiley; 2010. p. 581-598.